TECHNICAL REPORT BRL-TR-3342

BRL

A COUPLED POWER-PLASMA MODEL AND APPLICATION TO ELECTROTHERMAL-CHEMICAL GUNS

P. K. TRAN
G. P. WREN

MAY 1992

U.S. ARMY LABORATORY COMMAND

BALLISTIC RESEARCH LABORATORY
ABERDEEN PROVING GROUND, MARYLAND

NOTICES

Destroy this report when it is no longer needed. DO NOT return it to the originator.

Additional copies of this report may be obtained from the National Technical Information Service, U.S. Department of Commerce, 5285 Port Royal Road, Springfield, VA 22161.

The findings of this report are not to be construed as an official Department of the Army position, unless so designated by other authorized documents.

The use of trade names or manufacturers' names in this report does not constitute indorsement of any commercial product.

REPORT DOCUMENTATION PAGE

Form Approved
OMB No. 0704-0188

1. AGENCY USE ONLY (Leave blank)	2. REPORT DATE	3. REPORT TYPE AND DATES COVERED
	May 1992	Final, Jan 91-Dec 91

4. TITLE AND SUBTITLE

A Coupled Power-Plasma Model and Application to Electrothermal-Chemical Guns

5. FUNDING NUMBERS

PR: 1F2Z9W9XDGS3
DA311880

6. AUTHOR(S)

P. K. Tran and G. P. Wren

7. PERFORMING ORGANIZATION NAME(S) AND ADDRESS(ES)

8. PERFORMING ORGANIZATION REPORT NUMBER

9. SPONSORING/MONITORING AGENCY NAME(S) AND ADDRESS(ES)

U.S. Army Ballistic Research Laboratory
ATTN: SLCBR-DD-T
Aberdeen Proving Ground, MD 21005-5066

10. SPONSORING/MONITORING AGENCY REPORT NUMBER

BRL-TR-3342

11. SUPPLEMENTARY NOTES

12a. DISTRIBUTION/AVAILABILITY STATEMENT

Approved for public release; distribution is unlimited

12b. DISTRIBUTION CODE

13. ABSTRACT *(Maximum 200 words)*

A coupled power-plasma cartridge model of the electrothermal-chemical gun has been developed to investigate the dependence of plasma properties on the pulse-forming network (PFN) and on geometric variations. The model is validated against experimental data and parametrically varied to suggest the functional dependence of the plasma properties on the PFN and plasma components.

14. SUBJECT TERMS

electrothermal-chemical gun, propulsion systems, interior ballistics, plasma properties

15. NUMBER OF PAGES
33

16. PRICE CODE

17. SECURITY CLASSIFICATION OF REPORT	18. SECURITY CLASSIFICATION OF THIS PAGE	19. SECURITY CLASSIFICATION OF ABSTRACT	20. LIMITATION OF ABSTRACT
UNCLASSIFIED	UNCLASSIFIED	UNCLASSIFIED	UL

INTENTIONALLY LEFT BLANK.

TABLE OF CONTENTS

INTENTIONALLY LEFT BLANK.

LIST OF FIGURES

LIST OF TABLES

INTENTIONALLY LEFT BLANK.

ACKNOWLEDGMENT

The authors would like to thank J. Powell, T. Coffee, CPT K. Nekula, H. Burden, G. Katulka, and S. Richardson, U.S. Army Ballistic Research Laboratory, for their assistance and helpful suggestions at various stages of this project. The authors would also like to acknowledge the reviewers of the final manuscript, J. Powell and CPT K. Nekula.

INTENTIONALLY LEFT BLANK.

1. INTRODUCTION

The electrothermal-chemical (ETC) gun, generically shown in Figure 1, is a propulsion concept which utilizes a low mass, high energy plasma to initiate and, potentially augment and control the combustion/vaporization of the propellant (working fluid) during the ballistic cycle. The propulsion system has five major components: (1) the power supply; (2) the pulse-forming network (PFN) and switches; (3) the plasma generator; (4) the combustion chamber; and (5) the tube and projectile. Control of the interior ballistic (IB) process in terms of gas generation rate is theoretically accomplished by tailoring the delivery of electrical energy to the propellant in the combustion chamber in a manner to control combustion or vaporization of the propellant. Although the propellant may be liquid, gelled, or solid, the function of the plasma remains that of the initiator and controller.

In some design implementations, the plasma is formed in a plasma capillary (see Figure 1). In the rear capillary design, the dominant plasma properties believed to be important in the propellant combustion process are the energy, mass and velocity of the plasma entering the combustion chamber. These properties are shaped by the delivery of current from the PFN. Although the quantitative effects of variation of plasma mass, energy, and velocity on the combustion process are not known, it is of interest to determine the coupled effects of variation in the PFN and plasma cartridge geometry on the state of the plasma. These parametric relationships serve as a basis for design considerations.

In addition, it has been observed experimentally that unprogrammed changes in the coupled PFN-plasma subsystem occur which may affect the IB cycle. Shown in Figure 2 are power histories from ten 30-mm repeatability shots using a rear plasma capillary, and shown in Figure 3 are the electrical energy histories (integral of the power history) for the same series (FMC Corporation, Contract #DAAA21-88-C-0271). The repeatability series forms a sequence of shots in which the initial conditions are carefully controlled and all inputs are intended to be identical. However, the electrical energy variation in the plasma cartridge is seen to be 7%. For this series, the difference in maximum pressure is 13.3% and the muzzle velocity variation is 2.5%. The results are considered encouraging, although they do not meet the criteria of 0.5% standard deviation in muzzle velocity required for decision point 1 under the Electrical Enhancement Factor (EEF) ETC follow-on contracts (1991).

Under the current Army ETC cartridge development contracts (Oberle, private communication), the contractor is responsible for meeting the decision point criteria with a cartridge design consisting of the

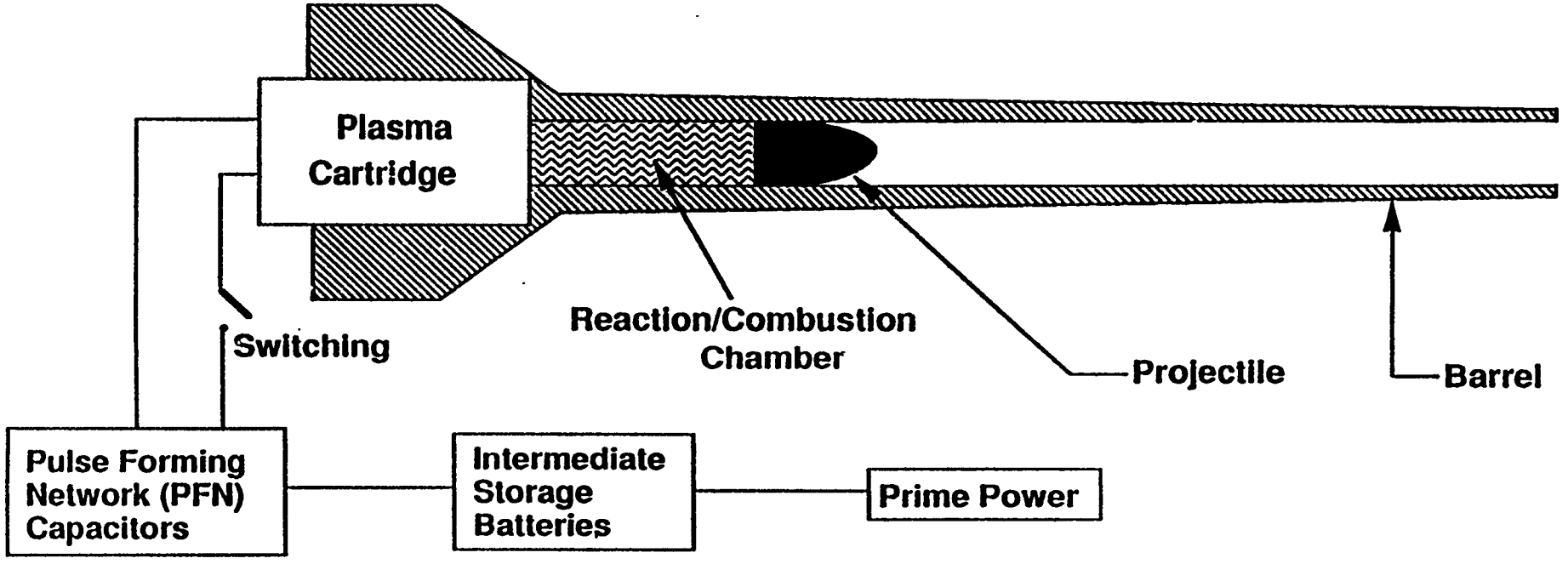

Figure 1. An Electrothermal-Chemical (ETC) Gun.

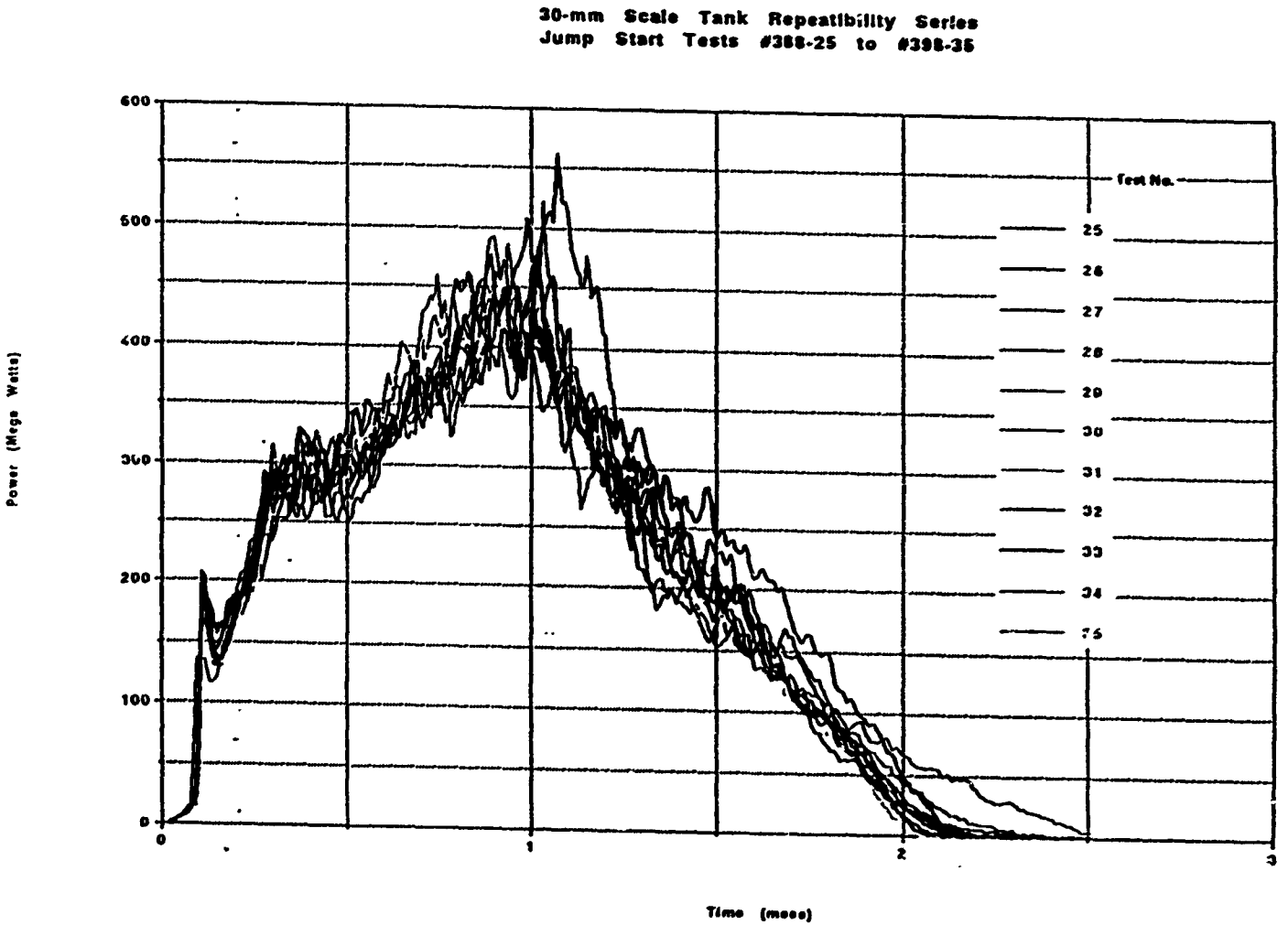

Figure 2. Power Histories From Ten 30-mm Repeatability Shots.

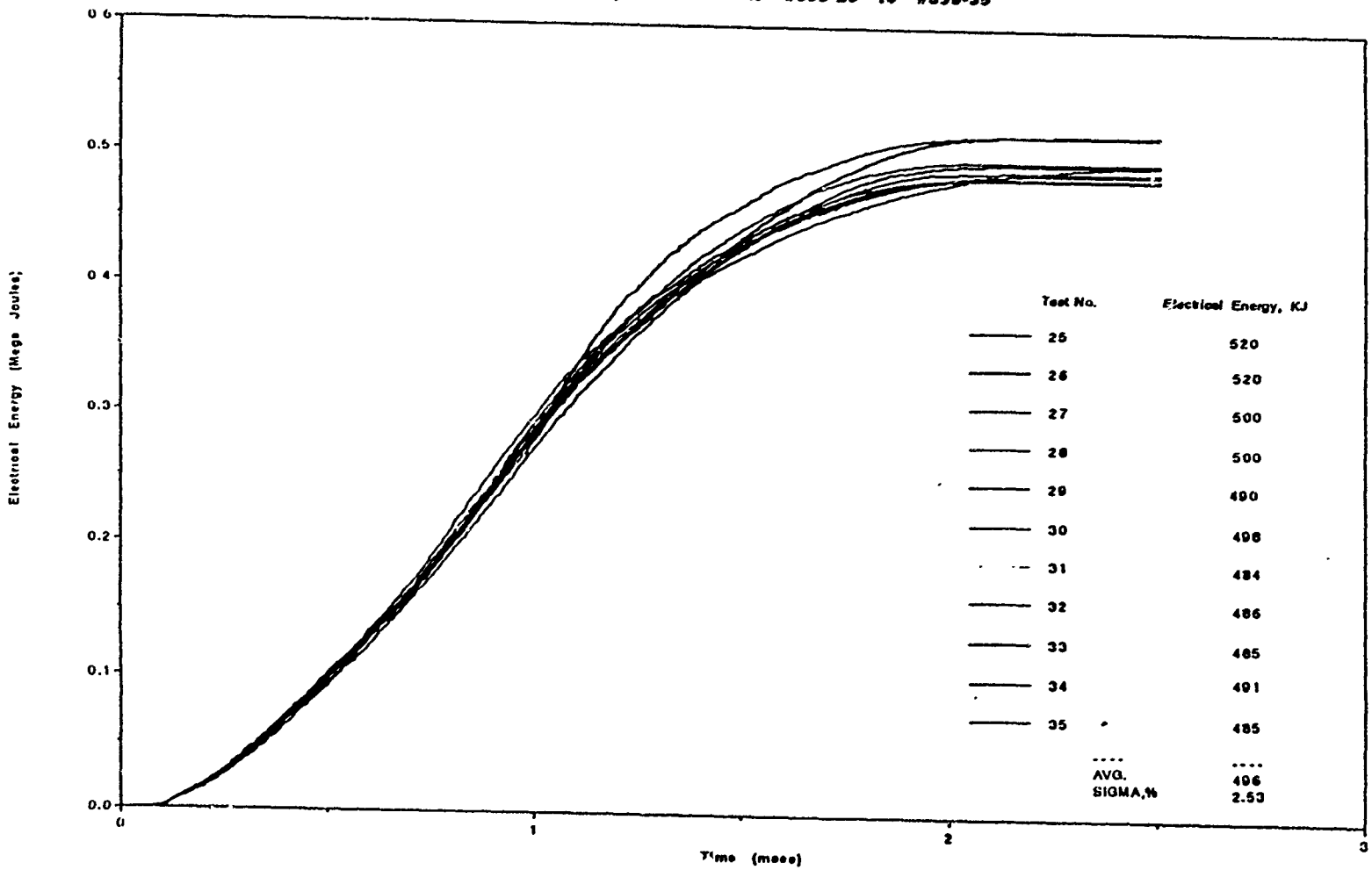

Figure 3. Electrical Energy Historics From Ten 30-mm Repeatability Shots.

plasma integrated into a propellant. The contractor is not responsible for the development and reliability of the power supply. Based on experimental data such as that shown in Figures 2 and 3, it might be expected that variation may occur in the PFN itself which may affect the plasma properties, subsequently affecting the interior ballistic cycle. If variability in the IB cycle can be directly related to variability in the PFN, then ballistic results in terms of pressures and muzzle velocity will need to be viewed in the context of the delivery of electrical energy.

Thus, the work presented in this paper has two objectives: (1) determine the sensitivity of the plasma properties to variations in the PFN; and (2) parametrically develop guidelines for modifications of plasma properties by changes in the PFN and geometry of the plasma cartridge. To accomplish the objectives, a coupled PFN-plasma cartridge model has been developed. The model is applied to and validated against the experimental fixture at the Ballistic Research Laboratory (BRL). Parametric variations of input to the PFN and geometry of the plasma cartridge are examined for the effect on the plasma properties.

2. PFN MODEL DESCRIPTION

The PFN model was developed by simulating the five-stage, 130-kJ PFN network in the ETC facility at BRL. The network consists primarily of five series of high energy capacitors, ignitrons, inductors, and resistors. Each module is triggered independently. The modules are connected directly to the anode and the cathode of the plasma capillary or to a fixed-metallic resistance, as shown in Figure 4.

In this circuit, the capacitors serve as energy storage and are clamped by the diodes to protect the capacitors from voltage reversals. The ignitrons are used as timed closing switches. The timed firing of the ignitrons and the characteristics of the resistor, induction, and capacitor (RIC) circuit change the shape and the duration of the current pulse. When the switch closes, the network is a voltage-fed network, and it becomes a current-fed network when the diode starts to conduct. The initially stored energy is equal to one-half of the total amount of capacitances in the circuit multiplied by the square of initial voltage charges across the capacitors,

$$E = \frac{1}{2} \sum_{i=1}^{5} C_i V_i^2 \ . \qquad (1)$$

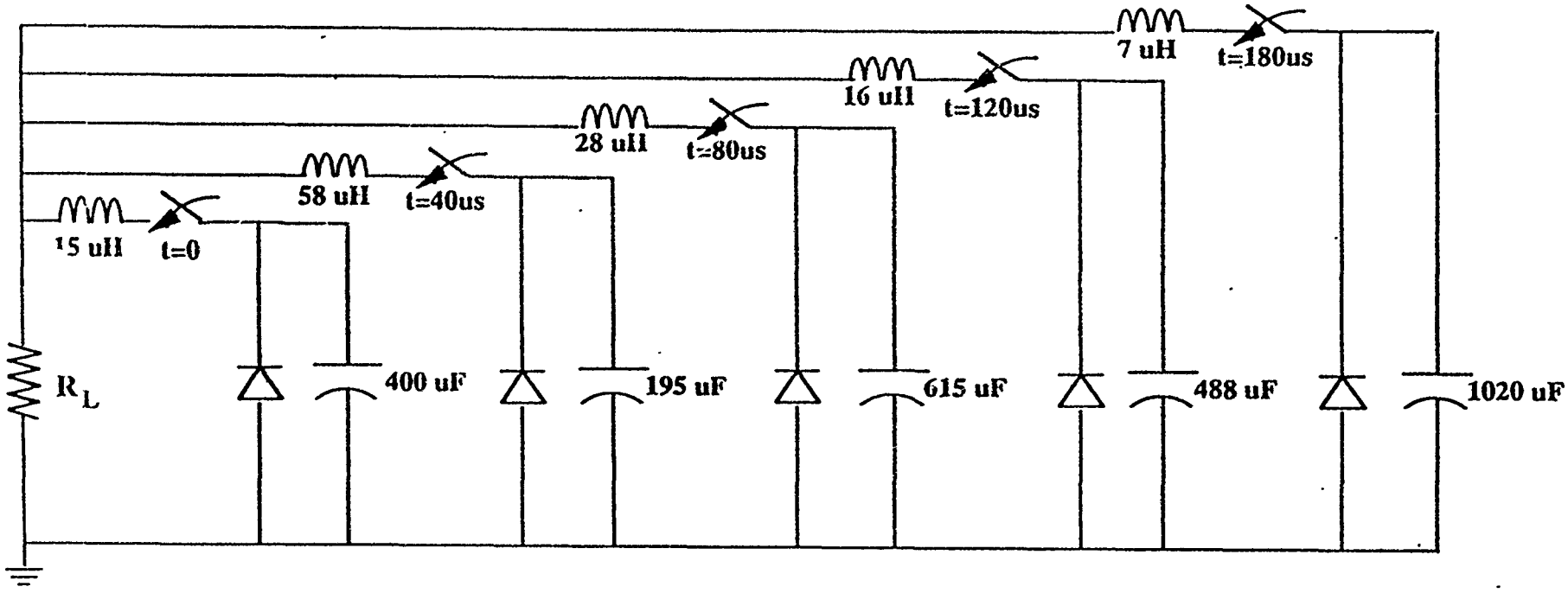

Figure 4. The BRL Five-Module, Pulse-Forming Network (135 kJ at 10 KV) for the ETC Gun.

The resultant current pulse through the load depends on the initial voltage charge across each capacitor, the values of capacitance, inductance, load resistance, and the closing times of the switches. To simplify the circuit analysis, it is assumed that there is no thermal effect on the network components. The capacitor is treated as a pure capacitor in series with a small resistor and an inductor; the inductor as in series with a small resistor, and the diode as in series with a resistor. The equations which are used in this PFN model are divided into two cases: (1) the circuit as a voltage fed-network; and (2) the circuit as a current-fed network.

Case 1: The circuit is a voltage fed network with each module treated as a simple loop RLC circuit.

The analysis of the circuit is based on the following equations. According to Kirchoff's law,

$$V_{ci} + V_{ri} + V_{li} + V_{load} = 0 \tag{2}$$

where V is voltage and the subscripts refer to the capacitance of the capacitor (ci), sum of the inductances (li), and sum of resistances (ri) in ith module, and the current of each module is

$$I_{ci} = I_{li} = I_i \, . \tag{3}$$

Voltage across the capacitor can also be defined as

$$V_{ci} = \frac{Q}{C} \tag{4}$$

where Q is the charge of the capacitor. The current through the capacitor is given by

$$I_{ci} = I_i = \frac{dQ}{dt} = C \frac{dV_{ci}}{dt} \, , \tag{5}$$

and the voltage across the inductance is defined by

$$V_{li} = L \frac{dI_i}{dt} . \tag{6}$$

The voltage across the load is given by

$$V_{load} = R_{load} I_{load} = R_{load} \sum_{i=1}^{5} I_i . \tag{7}$$

Substituting Equations 4, 5, 6, and 7 into Equations 2 and 3, and rearranging gives

$$\frac{dV_{ci}}{dt} = \frac{I_i}{C} \tag{8}$$

and

$$\frac{dI_i}{dt} = - \frac{V_{ci} + R_i I_i + R_{load} \sum_{i=1}^{5} I_i}{L_i} . \tag{9}$$

These two differential equations form the primary equations used in the PFN model.

Case 2: Current fed network, the circuit after the diode starts to conduct. It is assumed that the small current through the capacitor can be neglected, and the equations in this case are

$$V_d + V_{ri} + V_{li} + V_{load} = 0 \tag{10}$$

and

$$\frac{dI_i}{dt} = - \frac{V_d + R_i I_i + R_{load} \sum_{i=1}^{5} I_i}{L_i} \tag{11}$$

where *Vd* is forward diode voltage.

The plasma capillary model is a one-dimensional, steady-state, isothermal model which solves the basic magnetohydrodynamic conservation equations for the nonideal plasma, calculates the plasma conductivity, its ionization state, and approximate pertinent equations of state (Powell and Zielinski). Since the plasma model has a free boundary on the combustion chamber side, a "choked flow" assumption is utilized at the nozzle. That is, it is assumed that mass exits the nozzle at the local sound speed of the plasma.

Consequently, the linked PFN-plasma model is a feedback system where the output conductivity of plasma is used to calculate the input load resistance of the PFN. The output of the PFN model, which is the current across the capillary, is the input of plasma model.

3. MODEL VALIDATION

A comparison of the diagnostic data and model current output is carried out for both fixed-metallic load and plasma load. These experimental data were taken in September 1990 at BRL with the PFN shown in Figure 4 (Katulka, Burden, and Zielinski 1990). The rate of change of current through the load was measured by using a Rogowski probe. Due to the lack of information about the resistances and inductances of capacitors, they are assumed to be zero in the calculations.

With constant load (Table 1), the percent differences between the peak currents and the predicted results for the two experimental sets examined are 2% and 4%, considered to be reasonable agreement.

Table 1. Comparison With Experiment for Constant Load

	Set #1	Set #2
Initial voltage charge (KV)	1.0/C1-5	2.0/C1,3.0/C2-5
Total initial energy (kJ)	1.4	11.3
Switch closing times (μs)	0,180,270,497,641	0,180,270,497,641
Load resistance (mΩ)	35	35
Experimental max. current (KA)	9.9	32.1
Model max. current (KA)	10.1	30.8
Difference	+2%	-4%

In the case of a plasma capillary load, the coupled PFN-plasma model is run under the assumption of choked flow. The differences of peak currents for the two experimental data sets examined are 3% and 9% as shown in Table 2. The reason for the larger discrepancy between the model and data in Set 2 in Table 2 is not known.

Table 2. Comparison With Experiment for Plasma Load

	Set #3	Set #4
Initial voltage charge (KV)	2.0/C1,4.0/C2-5	2.0/C1,3.2/C2-5
Total initial energy (kJ)	19.5	12.8
Switch closing times (μs)	0,180,270,497,641	0,280,370,597,741
Capillary length (mm)	52.75	52.75
Capillary diameter (mm)	12.3	9.625
Experimental max. current (KA)	46.6	25.5
Model max. current (KA)	48.2	27.7
Difference	+3%	+9%

The current vs. time curves of the diagnostic record and the corresponding simulation for a constant load and a plasma load show good agreement as shown in Figures 5 and 6.

4. PARAMETRIC VARIATION

In order to evaluate the coupling between the PFN and the plasma capillary and the corresponding effect on plasma properties, the data set used for the validation in Section 3 was chosen as a baseline and parametrically varied. The data in Table 2, Set #3, with 19.5-kJ initial energy and with a capillary 52.75 mm long and 12.30 mm diameter were varied with a percentage change in (1) the initial voltage charge; (2) the capillary diameter; (3) the capillary length; and (4) the combination of changes in the diameter and the length of the plasma capillary in opposite directions. Thus, a change of +10% indicates an increase of 10% over the baseline in one initial condition with all other conditions the same as the baseline. A change of +10% in (4) indicates that the length increased by +10% and the diameter decreased by -10% over the baseline base. Corresponding changes in plasma properties examined were: (1) the load resistance at maximum current; (2) the maximum plasma current; (3) the total dissipated energy of the capillary; (4) the total plasma mass exit; and (5) the pressure at the end of capillary. The results are shown in Figures 7–11.

• Current vs Time (with constant load)

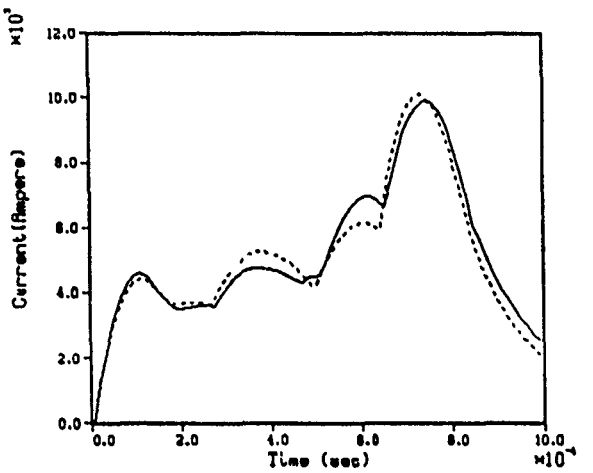

Line : experiment
Dot : BRL model

Figure 5. Current vs. Time With Constant Load (Data Set) #1).

• Current vs Time (with plasma load) *

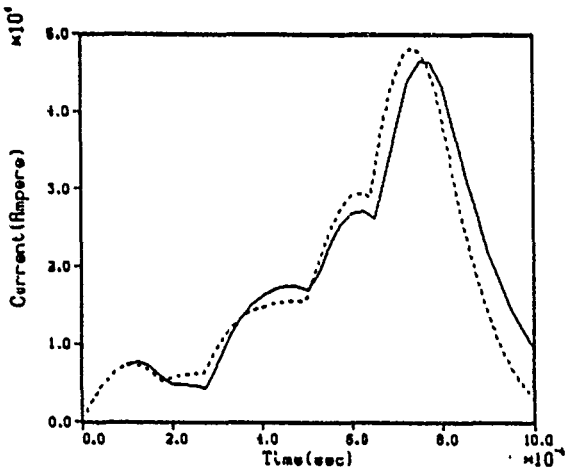

* Time varying resistance

Line : experiment
Dot : PFN-plasma model

Figure 6. Current vs. Time With Plasma Load (Data Set #3).

As indicated in Figures 7–11, the change in the initial voltage charge of the power supply is the most important factor, influencing all the important properties of plasma. The current across the load increases nearly linearly with the increase of the initial voltage charge across the capacitors (Figure 8). Voltage increases cause an increase in plasma temperature and plasma conductivity (Figure 7), consequently causing an increase in plasma current (Figure 8) and in the dissipated energy (Figure 9). Total plasma mass through the nozzle (Figure 10), and the breech pressure (Figure 11) also increase because the ablation rate increases with the temperature.

In the case of changing the capillary radius, the analysis is more complicated. The simulation output shows that the plasma properties are more sensitive to the changes in the radius than changes in the length. When the radius decreases 30%, the resistance of plasma at maximum current increases about 70% (Figure 7) and the breech pressure (Figure 11) increases 100%. Meanwhile, dissipated energy (Figure 9) and total plasma mass exit from the capillary (Figure 10) show insignificant change. However, when the capillary length increases, the plasma resistance linearly increases (Figure 7), with a resulting decrease in maximum current (Figure 8) across the capillary. The total dissipated energy (Figure 9) and the breech pressure (Figure 11) change only slightly from baseline in this case. However, the total mass exit (Figure 10) shows an increase of approximately 15% when the length increases 30%.

The worst case of changes in the resistance and the pressure should occur for the case when the radius increases and the length decreases or vice versa. If the radius decreases 20% and the length increases 20%, the resistance (Figure 7) increases about 80% and the pressure (Figure 11) increases about 60%. However, in this case the total mass exit (Figure 10) and total energy show only a slight change.

5. CONCLUSIONS

A coupled PFN-plasma capillary model has been developed for the experimental fixture at BRL. The model agrees well with baseline experimental data both for a fixed load and plasma load. Parametric variation of various input parameters suggest that, compared to the baseline:

(1) total plasma dissipated energy and mass are most sensitive to changes in initial voltage;

(2) total plasma dissipated energy and mass are not strongly affected by changes in the plasma capillary geometries considered;

(3) changes of 5% variation (on the order observed in the experimental firings) in the initial voltage yield changes of 9% in total plasma dissipated energy and 7% in total plasma mass at the exit; and

(4) pressure at the nozzle is strongly affected by both initial voltage and capillary radius.

The effect on gun performance (in terms of maximum pressure and muzzle velocity) of the coupling of variations in plasma mass, energy and momentum with an energetic propellant was not investigated and remains a subject for future investigation.

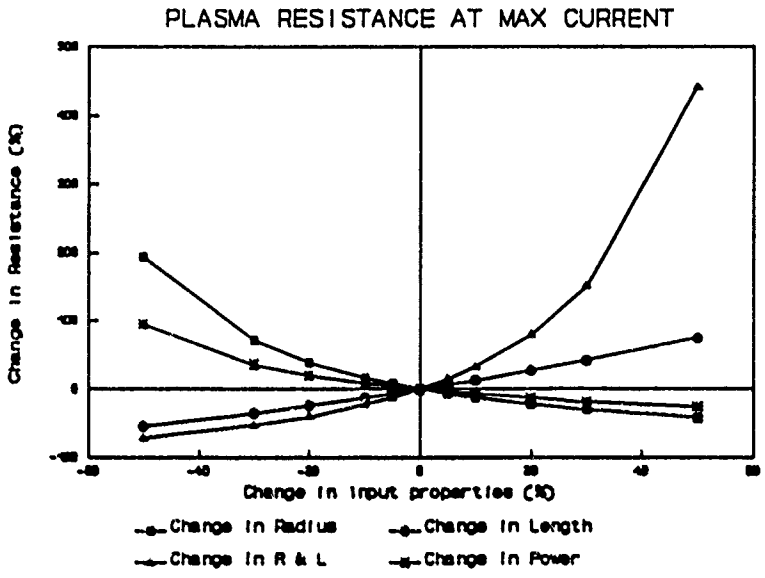

Figure 7. Plasma Resistance at Max Current as a Function of Parametric Variation.

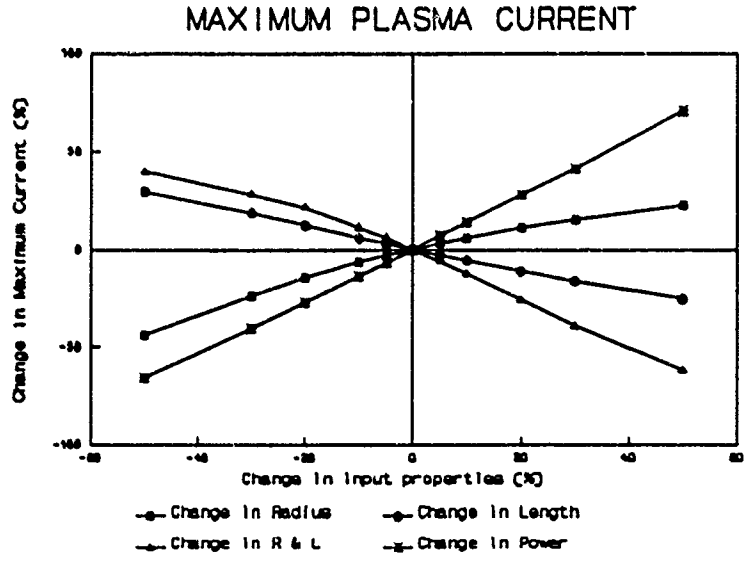

Figure 8. Maximum Plasma Current as a Function of Parametric Variation.

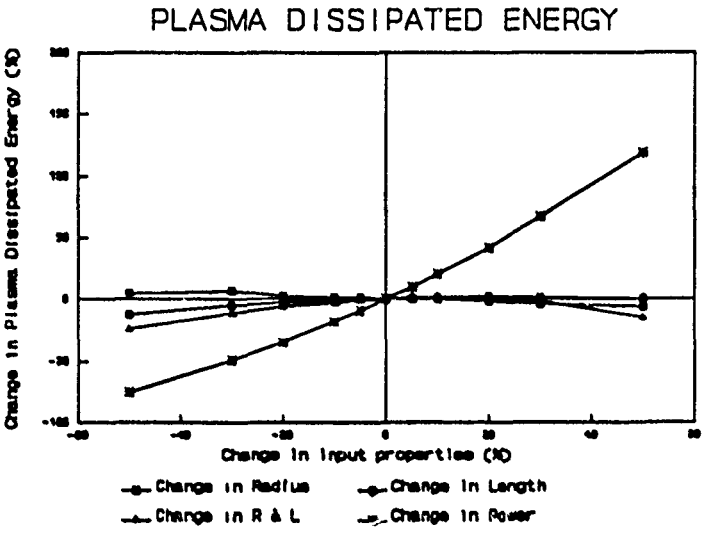

Figure 9. Plasma Dissipated Energy as a Function of Parametric Variation.

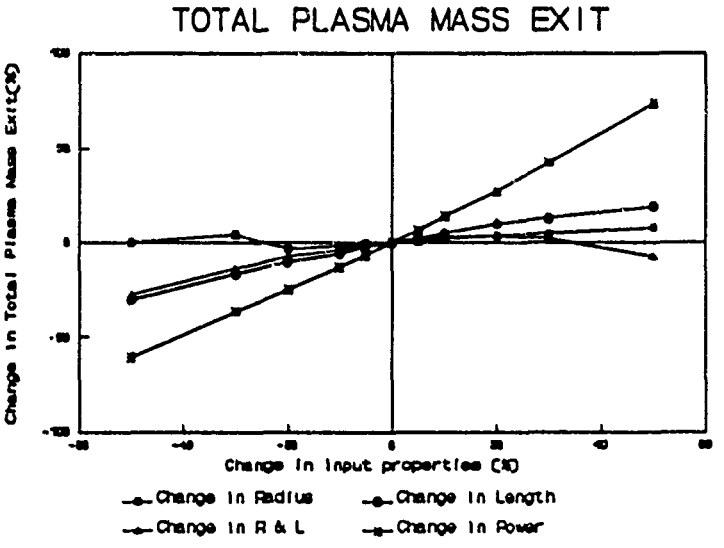

Figure 10. Plasma Mass Exit as a Function of Parametric Variation.

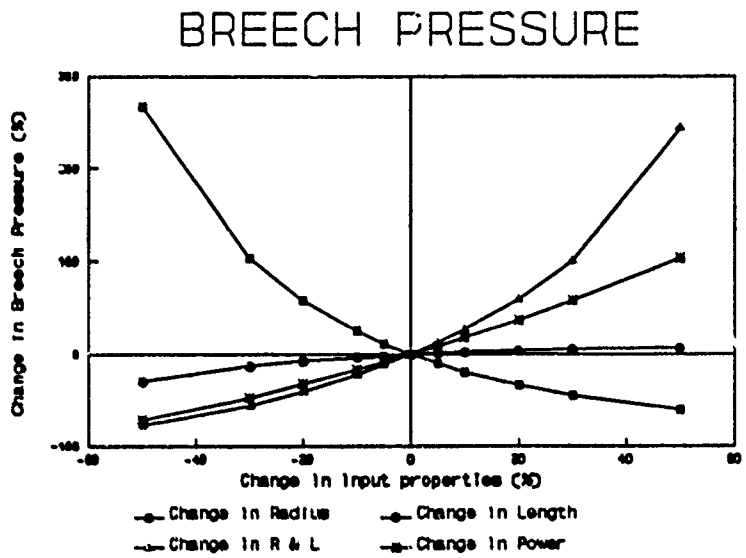

Figure 11. Breech Pressure as a Function of Parametric Variation.

6. REFERENCES

FMC Corporation, Contract DAAA21-88-C-0271.

Katulka, G. L., H. Burden, A. Zielinski, and K. White. "Electrical Energy Shaping for Ballistic Applications in ET Gun." Technology Efforts in ETC Gun Propulsion, vol. 3, FY 90, Ballistic Research Laboratory, Aberdeen Proving Ground, MD, December 1990.

Oberle, W. F. ETC Technology Program Coordinator, Ballistic Research Laboratory, private communication.

Powell, J. D., and A. E. Zielinski. "Theory and Experiment for an Ablating Capillary Discharge and Application to Electrothermal-Chemical Guns." Ballistic Research Laboratory Report, to be published.

Rashid, M. H. Power Electronics, Prentice-Hall, Inc. 1988.

"U.S. Army ETC Technology Objectives," Ballistic Research Laboratory memorandum, January 1991.

INTENTIONALLY LEFT BLANK.

No. of Copies	Organization
2	Administrator Defense Technical Info Center ATTN: DTIC-DDA Cameron Station Alexandria, VA 22304-6145
1	Commander U.S. Army Materiel Command ATTN: AMCAM 5001 Eisenhower Ave. Alexandria, VA 22333-0001
1	Commander U.S. Army Laboratory Command ATTN: AMSLC-DL 2800 Powder Mill Rd. Adelphi, MD 20783-1145
2	Commander U.S. Army Armament Research, Development, and Engineering Center ATTN: SMCAR-IMI-I Picatinny Arsenal, NJ 07806-5000
2	Commander U.S. Army Armament Research, Development, and Engineering Center ATTN: SMCAR-TDC Picatinny Arsenal, NJ 07806-5000
1	Director Benet Weapons Laboratory U.S. Army Armament Research, Development, and Engineering Center ATTN: SMCAR-CCB-TL Watervliet, NY 12189-4050
(Unclass. only) 1	Commander U.S. Army Rock Island Arsenal ATTN: SMCRI-TL/Technical Library Rock Island, IL 61299-5000
1	Director U.S. Army Aviation Research and Technology Activity ATTN: SAVRT-R (Library) M/S 219-3 Ames Research Center Moffett Field, CA 94035-1000
1	Commander U.S. Army Missile Command ATTN: AMSMI-RD-CS-R (DOC) Redstone Arsenal, AL 35898-5010

No. of Copies	Organization
1	Commander U.S. Army Tank-Automotive Command ATTN: ASQNC-TAC-DIT (Technical Information Center) Warren, MI 48397-5000
1	Director U.S. Army TRADOC Analysis Command ATTN: ATRC-WSR White Sands Missile Range, NM 88002-5502
1	Commandant U.S. Army Field Artillery School ATTN: ATSF-CSI Ft. Sill, OK 73503-5000
2	Commandant U.S. Army Infantry School ATTN: ATZB-SC, System Safety Fort Benning, GA 31903-5000
(Class. only) 1	Commandant U.S. Army Infantry School ATTN: ATSH-CD (Security Mgr.) Fort Benning, GA 31905-5660
(Unclass. only) 1	Commandant U.S. Army Infantry School ATTN: ATSH-CD-CSO-OR Fort Benning, GA 31905-5660
1	WL/MNOI Eglin AFB, FL 32542-5000
	Aberdeen Proving Ground
2	Dir, USAMSAA ATTN: AMXSY-D AMXSY-MP, H. Cohen
1	Cdr, USATECOM ATTN: AMSTE-TC
3	Cdr, CRDEC, AMCCOM ATTN: SMCCR-RSP-A SMCCR-MU SMCCR-MSI
1	Dir, VLAMO ATTN: AMSLC-VL-D
10	Dir, USABRL ATTN: SLCBR-DD-T

No. of Copies | Organization

1 Commander
U.S. Army Armament Research,
Development, and Engineering Center
ATTN: Ms. Hildi Naber-Libby
Bldg. 329
Picatinny Arsenal, NJ 07806-5000

1 Commander
U.S. Army Armament Research,
Development, and Engineering Center
ATTN: Dr. Arthur Bracuti
Bldg. 382
Picatinny Arsenal, NJ 07806-5000

1 Commander
U.S. Army Armament Research
Development, and Engineering Center
ATTN: Mr. Donald Chiu
Bldg. 382
Picatinny Arsenal, NJ 07806-5000

1 Commander
U.S. Army Armament Research,
Development, and Engineering Center
ATTN: Dr. David Downs
Bldg. 382
Picatinny Arsenal, NJ 07806-5000

1 Director
U.S. Army Armament Research,
Development, and Engineering Center
Benet Weapons Laboratory
ATTN: SMCAR-CCB-RA, G. Carafano
Watervliet, NY 12189-4050

1 Commander
Naval Sea Systems Command
Department of the Navy, CSEA 06 KR12
ATTN: CDR Craig Dampier
Washington, DC 20362-5101

2 Deputy Commander USASDC
ATTN: SFAE-SD-HVL, Mr. Stan Smith
P.O. Box 1500
Huntsville, AL 35887-38011

No. of Copies | Organization

1 Director
Sandia National Laboratories,
Combustion Research Facility
Energetic Materials Division 8357
ATTN: Dr. Robert Armstrong
Livermore, CA 94551-0969

1 Director
Sandia National Laboratories
Advanced Projects Division 9123
ATTN: Dr. David Benson
Albuquerque, NM 87185-5800

2 Director
Sandia National Laboratories
Advanced Projects V
ATTN: Dr. Steve Kempka
Dr. Ronald Woodfin
Albuquerque, NM 87185-5800

1 Director
Sandia National Laboratories
Imaging Technology Division
ATTN: Dr. Donald Sweney
Livermore, CA 94551-0969

1 Director
Sandia National Laboratories
Division 8357
ATTN: Dr. Steven Vosen
Livermore, CA 94551-0969

2 State University of New York
ATTN: Dr. W. J. Sarjeant
Prof. James Clark Maxwell
Dept. of Electrical Engineering
Bonner Hall—Room 312
Buffalo, NY 14260

1 The Pennsylvania State University
Dept. of Mechanical Engineering
ATTN: Dr. Kenneth Kuo
140 Research Building East
University Park, PA 16802

1 North Carolina State University
ATTN: Dr. John Gilligan
Campus Box 7909
Raleigh, NC 27695-7909

No. of Copies | Organization

1 GT-Devices, Inc.
ATTN: Dr. Joseph R. Greig
5705A General Washington Drive
Alexandria, VA 22312

1 GT-Devices, Inc.
ATTN: Dr. Neils Winsor
5705A General Washington Drive
Alexandria, VA 22312

3 FMC Corporation
Northern Ordnance Division
ATTN: Dr. Anthony Giovanetti
Dr. David Cook
Mr. John Dvyik
4800 East River Road
Minneapolis, MN 55421

2 Science Applications International Co.
ATTN: Mr. Neeraj Sinha
Dr. Sanford Dash
501 Office Center Drive, Suite 420
Fort Washington, PA 19034-3211

2 Science Applications International Co.
ATTN: Dr. Jad Batteh
Mr. Lindsey Thornhill
1519 Johnson Ferry Road, Suite 300
Marietta, GA 30062

1 Alliant Techsystems Inc.
ATTN: Mr. James Kennedy
7225 Northland Drive
Brooklyn Park, MN 55428

1 Princeton Combustion Research
Laboratories, Inc.
ATTN: Dr. N. A. Messina
4275 U.S. Highway One North
Monmouth Junction, NJ 08852

No. of Copies | Organization

1 Olin Ordnance
ATTN: Mr. Hugh A. McElroy
10101 9th Street North
St. Petersburg, FL 33716

1 Freedman Associates
ATTN: Dr. Eli Freedman
2411 Diana Road
Baltimore, MD 21209-1525

1 Paul Gough Associates, Inc.
ATTN: Dr. Paul Gough
1048 South Street
Portsmouth, NH 03801

No. of Copies	Organization
1	RARDE GS2 Division Building R31 ATTN: Dr. Clive Woodley Fort Halstead Sevenoaks, Kent TN 14 7BT England

USER EVALUATION SHEET/CHANGE OF ADDRESS

This laboratory undertakes a continuing effort to improve the quality of the reports it publishes. Your comments/answers below will aid us in our efforts.

1. Does this report satisfy a need? (Comment on purpose, related project, or other area of interest for which the report will be used.) _____

2. How, specifically, is the report being used? (Information source, design data, procedure, source of ideas, etc.) _____

3. Has the information in this report led to any quantitative savings as far as man-hours or dollars saved, operating costs avoided, or efficiencies achieved, etc? If so, please elaborate. _____

4. General Comments. What do you think should be changed to improve future reports? (Indicate changes to organization, technical content, format, etc.) _____

BRL Report Number BRL-TR-3342 Division Symbol _____

Check here if desire to be removed from distribution list. ____

Check here for address change. ____

Current address: Organization _____
Address _____

DEPARTMENT OF THE ARMY
Director
U.S. Army Ballistic Research Laboratory
ATTN: SLCBR-DD-T
Aberdeen Proving Ground, MD 21005-5066

OFFICIAL BUSINESS

BUSINESS REPLY MAIL
FIRST CLASS PERMIT No 0001, APG, MD

Postage will be paid by addressee

Director
U.S. Army Ballistic Research Laboratory
ATTN: SLCBR-DD-T
Aberdeen Proving Ground, MD 21005-5066

NO POSTAGE
NECESSARY
IF MAILED
IN THE
UNITED STATES